XVII[èmes] Journées Nationales Génie Côtier – Génie Civil
Chatou, 2022
DOI:10.5150/jngcgc.2022.003 *© Editions Paralia CFL*
disponible en ligne – http://www.paralia.fr – available online

Drivers of tidal characteristic changes in north western France: a statistical analysis

Jack CHALLIS [1,2], Déborah IDIER [1], Guy WOPPELMANN [2], Gaël ANDRE [3], Raphaël LEGOUGE [3], Jérémy ROHMER [1]

1. BRGM, DRP/R3C, 3 avenue Claude Guillemin, 45060, Orléans, France.
   j.challis@brgm.fr ; d.idier@brgm.fr ; j.rohmer@brgm.fr
2. La Rochelle Université, LIENSs, 2 Rue Olympe de Gouges, 17000 La Rochelle, France.
   jack.challis@etudiant.univ-lr.fr; guy.woppelmann@univ-lr.fr
3. SHOM, 13 Rue de Châtellier, 29200 Brest, France.
   gael.andre@shom.fr ; raphael.legouge@shom.fr

Abstract:
Tides are changing on human timescales, and an understanding of reasons for these changes is important for inundation risk assessments and coastal defence planning. Tides are often regarded as astronomically generated phenomena, however recently published literature has investigated changes in tidal characteristics driven by non-astronomical factors. Physical mechanisms of many of these drivers are well understood, however studies assess the impact of a single or limited number of drivers. As such the relative impacts of these drivers are yet unknown. This work aims to investigate the medium to long-term tidal amplitude changes in relation to potential drivers. A statistical approach was developed, and applied to tide gauge data from Brest, Le Conquet, Saint-Malo and Dunkerque. This approach is designed to conduct comparative model fit analysis between competing multivariate linear regression models of tidal characteristics. The five main potential causes of tidal change investigated were: mean sea level, pressure-driven atmospheric storm surge, wind, waves and stratification. Annual mean and standard deviation are considered for storm surge, wind and wave data in order to represent the average value over the year and the intra-annual variability. Models of constituent amplitudes were constructed using every combination of drivers. The best models were selected using the Bayesian Information Criterion, and models displaying a negative R^2 or non-significant correlation were discarded. The results suggest the inverse barometer effect (a proxy of atmospheric storm surges) to be among the most commonly occurring drivers in models of tidal amplitudes for all 4 sites. These preliminary results will be further investigated using a hydrodynamic modelling approach.

Keywords: Tides, Tide change, Tidal constituents, Storm Surges, Climate change.

1. Introduction

It has been of scientific consensus for some time that tides are changing over human timescales due to non-astronomical phenomena (HAIGH *et al.*, 2020). As tides make up part of extreme sea levels, identifying the causes of these changes is crucial for understanding future inundation risks, as well as for predicting changes in sediment mobility and coastal erosion. There have been several studies that have sought to identify the impacts of non-astronomical changes on tides (HAIGH *et al.*, 2020, and references therein), and the physical mechanisms behind these interactions is in some cases very well understood. However these studies have currently focused only on singular causes or small groups of drivers (e.g. COLOSI & MUNK, 2006; HASHEMI *et al.*, 2015; IDIER *et al.*, 2017). The aim of this work is therefore (1) to identify potential causes of tidal change, and (2) determine the relative contributions of identified drivers. In this project, we focus on the following drivers: Mean Sea Level (MSL), wave power (P), wind speed squared (U^2), inverse barometer effect (IB) and stratification (ρ_{200}). Among the chosen drivers, the effects of changing MSL are the most well studied (e.g PELLING *et al.*, 2013; PELLING & GREEN, 2014; IDIER *et al.*, 2017). Rising MSL can affect tidal characteristics through a number of processes including changing resonant properties of the basin and bed friction (IDIER *et al.*, 2017). Inundation resulting from MSL change can also change tides, as energy dissipation can be spread across newly inundated areas (PELLING *et al.,* 2013). Wave power is also investigated as a cause. It has been shown that an increase in bed friction resulting from an increasingly energetic wave climate, in addition to excess momentum flux caused by the presence of waves can lead to a decrease in tidal currents (HASHEMI *et al.*, 2015). Wind speed was identified as a possible cause as wind directly interacts with tidal elevations through advection terms in the shallow water equations (HAIGH *et al.*, 2020). The justification for the inclusion of this driver is similar to that of wind, as both wind and pressure directly interact with tidal elevations through advection terms in the shallow water equations. It has also been noted that storm surges change bed friction (IDIER *et al.*, 2012). Stratification is also considered, as it is known that a more (less) stratified water column transfers energy from the barotropic to baroclinic tide, reducing baroclinic tidal amplitude (COLOSI & MUNK, 2006). This paper is structured as follows. Firstly section 2 describes the data used and outlines the developed approach. Results are presented in section 3. Section 3.1 covers detected tidal changes, whilst 3.2 displays the results of multivariate linear modelling. The final section discusses the implications of the results and the limitations of the approach.

2. Data and methods

2.1 Data

Tidal data. Validated hourly tide gauge data was obtained from the Service Hydrographique et Océanographique de la Marine (SHOM) for 4 sites: Brest, Le

Conquet, Dunkerque and Saint-Malo. These study sites were selected for individual reasons. Brest was selected as it is the longest tide gauge record in France. Le Conquet was selected due to its proximity to Brest. Dunkerque was selected as it is subject to strong instantaneous tide-surge interactions (IDIER *et al.*, 2012), and Saint-Malo as a site sensitive to MSL changes (e.g. IDIER *et al.*, 2017). 176, 52, 66 and 32 years of data were obtained for Brest, Le Conquet, Dunkerque Saint-Malo respectively.

Driver data. Table 1 presents a summary of all the datasets used in this research.

Table 1. Summary of all data used in this research.

	Water level	***Pressure***	***Wind***	***Waves***	***Stratification***
Original dataset	*Tide gauge*	*ERA5 reanalysis***			*Density anomaly profiles*
Provider	*SHOM*	*Copernicus*			*Yamaguchi and Suga (2019)*
Δx (Spatial)	*NC*	*0.25° x 0.25°*	*0.5° x 0.5°*		*5° x 10°*
Δt (Time)	*1h*	*1 month*			*1 year*
t_0 (start date)	*01/04/1846*	*01/01/1950*			*1960*
t_n (end date)	*01/01/2021*	*01/01/2021*			*2017*
t_n-t_0 (Record length)	*176 years (Brest)** *52 years (Le Conquet)* *66 years (Dunkerque)* *32 years (Saint-Malo)*	*71 years*			*57 years*
Location					
Brest	*48.38°N, 4.49°W*	*48.25°N, 5.25°W*	*48.0°N, 5.5°W*		*47.5°N, 5.0°W*
Le Conquet	*48.36°N, 4.78°W*				
Dunkerque	*52.5°N, 5.0°E*	*51.25°N, 2.50°E*	*51.53°N, 2.49°E*		*52.5°N, 5.0°E*
Saint-Malo	*48.64°N, 2.03°W*	*48.64°N, 2.03°W*			*NC*
Processing	*Tidal harmonic analysis*	*Yearly $\bar{x}$*	*Yearly $\bar{x}$ and σ_x of* $-\frac{P_A - \overline{P_A}}{\rho g}$	*Yearly $\bar{x}$ and σ_x of* $\boldsymbol{U^2}$	*Yearly $\bar{x}$ and σ_x of* $H_s{}^2 T_p$	*None*
Final dataset	CST_{amp}	*MSL*	$\overline{IB}$ σ_{IB}	$\overline{U^2}$ σ_{U^2}	$\overline{W}$ σ_W	$\Delta\rho_{200}$

*Note: NC Not Concerned; $\bar{x}$ Mean; σ_x Standard deviation; ***** Gaps in dataset; ** For information on ERA5 reanalysis see (HERSBACH et al., 2020).*

2.2 Method

A core principal of this approach lies in the process of Tidal Harmonic Analysis (THA), on a sliding annual scale window (POUVREAU *et al.*, 2006; RAY, 2006; MÜLLER, 2011). As a preliminary step, to ensure that the data obtained from the THA are of high quality, data filters in the literature (WOODWORTH *et al.*, 1991; POUVREAU *et al.*, 2006; WOODWORTH, 2010) were tested and applied. As a result, only years containing at least 11 months of continuous data were considered.

The UTide (CODIGA, 2011) THA package was used to retrieve annual amplitude values. A search list must be established to ensure consistency among the detected constituents for each year. A first pass of this moving window THA approach was applied, where UTide was allowed to retrieve any constituents for which the Signal to Noise Ratio (SNR) was greater than 2. Then a second pass is conducted searching only for tidal constituent present at every year in the preliminary pass. During this phase, gaps in data are discarded rather than interpolated and only the present data is analysed.

In order to identify multiple causes of tidal change and their relative impacts, multivariate linear models for the tidal amplitude changes of each constituent were constructed using every possible combination of drivers, in the following form:

$$\Delta CST_{amp} = \alpha \Delta x_1 + \beta \Delta x_2 \ldots \quad (1)$$

where: ΔCST_{amp} is the change in tidal amplitude for a given constituent (CST), Δx_1 and Δx_2, represent change in a driver dataset, and α and β are coefficients. Change is defined as the difference between a data point at time, t and the data value at the first-time step t_0.

Once every possible tidal model had been established, the standard formulation of the Bayesian Information Criterion (BIC) (SCHWARTZ, 1978) was used to determine the best model

$$BIC = k\, ln(n) - 2\, ln(\hat{L}) \quad (2)$$

where: n is equal to the number of observations datapoints, k is equal to the number of regressors, and $\hat{L}$ is likelihood function, which is defined as:

$$\hat{L} = f(y = (y_1, y_2, \ldots, y_n) | \hat{\theta}) \quad (3)$$

where: f denotes the probability density function that specifies the probability of observing data vector *y* given the vector of the linear regression model's parameters, i.e. $\hat{\theta} = (\alpha, \beta, \ldots)$.

Using the BIC for model selection addresses the problem of overfitting by penalising models that are more complex. When analysing the BIC value, it is the lowest BIC value that represents the best fitting model. However, by analysing solely the model with the lowest BIC model, there is a risk of interpreting models that physically make no sense. Therefore, it is important to consider how close the BIC value is to the next lowest value. If the second or third lowest values are all close to the first value, it may indicate that these models are worth interpreting in addition to that with the lowest BIC. A significance level of $p>0.05$ was used. In addition, the coefficient of determination R2 is also

considered. A negative R^2 value indicates that a model fits observational data worse than a regression model that corresponds to the mean of the dataset. Therefore, models displaying negative R^2 values are discarded.

3. Results

3.1 Tide changes

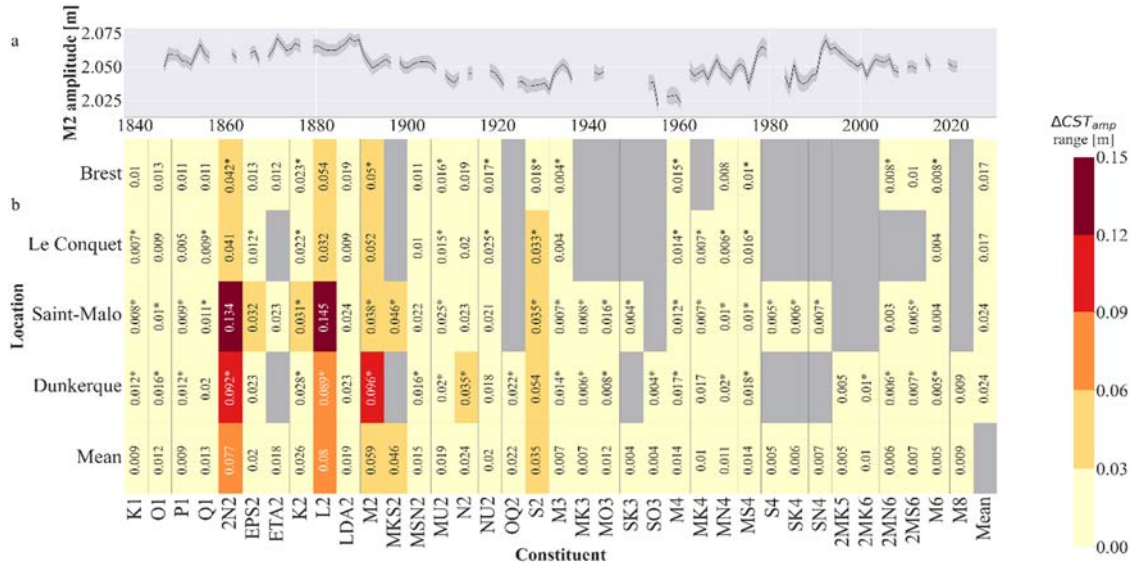

*Figure 1. (a) absolute M2 amplitude change at Brest since 1846; (b) Range of ΔCST_{amp} (where * represents statistically significant (p>0.05) models that also positive R^2 values).*

Figure 1a shows M2 amplitudes at Brest, and 1b shows the difference between the maximum and minimum amplitude detected for each constituent, including means over sites (rows) and constituents (columns).

In terms of constituents, L2 displays the largest difference among all sites, showing mean range of 0.08m (figure 1b, last row). L2 also displays the largest difference at any individual site, showing 0.145m of difference in Saint-Malo. In discussing constituents that show the smallest difference, SK3 and SO3 both show differences of 0.004m. The smallest difference at any individual site can be seen to be 2MN6, with a difference of 0.003m at Saint-Malo. Overall Dunkerque and Saint-Malo show the largest difference amongst all study sites (figure 1b, last column), both displaying a mean value of 0.024m. The mean ranges of change for Brest and le Conquet are both 0.017m. Among the constituents that are significant at every site, K2 is notable, as it is the largest, showing 0.026m mean difference.

3.2 Statistical models

The model of K2 and Brest (figure 2a.) largely follows the pattern of change showing in the observed changes. However, the model does not follow large spikes (both positive and negative) that occur throughout the 1960's to 1980's, showing discrepancies of up to 0.01m (for example as can be seen in 1978). The fit of the model appears to improve starting in the 1990's, following observed trends much more closely until the model finishes in 2017. The contributions to this model (figure 2c.) can be seen to be made up of both inverse barometer mean and standard deviation. It can be seen that whilst inverse barometer tends to follow the general pattern of the observed changes, the standard deviation of the inverse barometer is more effective in capturing the period of larger change such as the dip in 1976 and the spike in 2000.

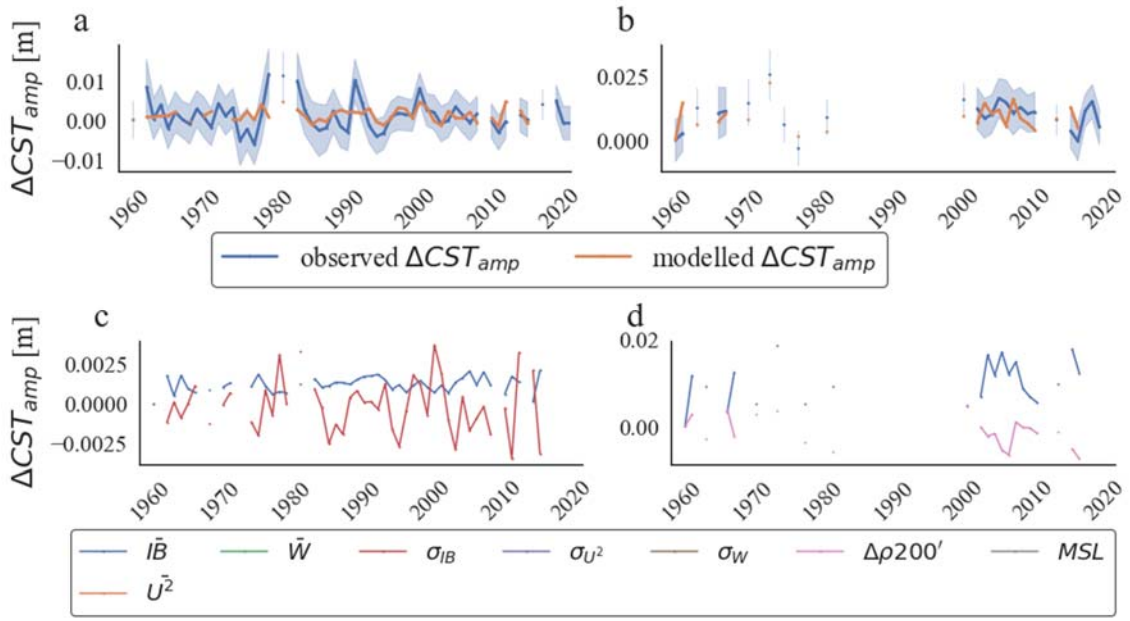

Figure 2. Best fitting model plotted against observation (a and b) for K2 amplitudes and diver contributions (c and d) at Brest and Dunkerque, (where blue shading shows upper/lower confidence levels for ΔCST_{amp}).

The K2 model for Dunkerque (figure 2b.) shows the same magnitude as the observations. Contrary to the behaviour of the K2 model at Brest (figure 2a.), which generally shows much smaller changes than the observation, the model at Dunkerque shows many periods of larger than observed change. Examples of this can be seen between 1960 and 1961, where the observed and modelled change both rise, but with modelled change rising to a larger value. In the period of 2000 to 2010, the model appears in most cases to rise and fall when the observations fall and rise respectively. The contributions of this model (figure 2d.) are made up of the inverse barometer mean and stratification. It is observable

throughout most of the modelled period that the contributions of stratification mirror those of the inverse barometer, rising when the other falls (and vice versa).
Beyond the displayed models, it was found among all significant models at all 4 study sites (notated in figure 1b. by *), the mean of the inverse barometer was one of the most commonly occurring drivers. The inverse barometer occurs the most commonly in Dunkerque, occurring in 13 out of the 22 significant models at this site. The least commonly occurring driver was found to be stratification, influencing only 2 constituent models at both Brest and Dunkerque. As such, this methodology was reapplied over the same period excluding stratification. This was found to have little impact on the occurrence of the drivers, reconfirming the dominance of the mean inverse barometer over this period.

4. Conclusion

Within this investigation of tidal components changes and the potential drivers, we found that Dunkerque and Saint-Malo exhibited the largest mean difference (0.024 m ; among all tidal components together) than those of Brest and Le Conquet (0.017m). L2 was found to have the largest difference among all 4 sites (figure 1b, last row), showing means of 0.08m, and also showing the largest overall range in Saint-Malo (0.145m).
The best fitting model for K2 at Brest and Dunkerque (figures 2a and 2b), along with the relative contributions of drivers to these models (figures 2c and 2d). The K2 constituent arises due to the declination of the moon and sun. It can be noted that $(IB)^{-}$is present in both of the displayed models. Beyond the displayed models, it was found that the mean of the inverse barometer was found to be one of the most commonly occurring drivers among statistically significant constituent amplitude models at all sites. This methodology was further tested by removing stratification and maintaining the same model period, the results of which reconfirmed the prominence of the inverse barometer in the models.
A limit of this approach is that it searches only for multivariate linear models, and does not account for non-linear interactions between drivers and tidal change, or driver intercorrelation. Investigations considering non-linear interactions may constituent a line of future research.
In conclusion, this research suggests that tide-surge interactions may be the principal driver of tidal amplitude change over the studied multi decadal time span (focusing on changes on a yearly resolution) amongst the 4 study sites. Hydrodynamic modelling work will be carried out in order to further investigate this relationship.

5. References

CODIGA D. (2011). *Unified tidal analysis and prediction using the UTide Matlab functions*. Narragansett. ftp://www.po.gso.uri.edu/pub/downloads/codiga/pubs/2011Codiga-UTide-Report.pdf
COLOSI J.A., MUNK W. (2006). *Tales of the venerable Honolulu tide gauge*, Journal of

Physical Oceanography, 36(6), pp 967–996. doi:10.1175/JPO2876.1

HAIGH I.D., PICKERING M.D., GREEN J.A.M., *et al.* (2020). *The tides they are a-changin: A comprehensive review of past and future nonastronomical changes in tides, their driving mechanisms, and future implications*', Reviews of Geophysics, 58(1), pp 1–39. doi:10.1029/2018RG000636

HASHEMI M.R., NEILL S.P., ROBINS E., DAVIES A.G., LEWIS M.J. (2015). *Effect of waves on the tidal energy resource at a planned tidal stream array*, Renewable Energy, 75, pp 626–639. doi:10.1016/j.renene.2014.10.029

HERSBACH H., BELL B., BERRISFORD P., *et al.* (2020). *The ERA5 global reanalysis*, Quarterly Journal of the Royal Meteorological Society, 146(730), pp 1999–2049. doi:10.1002/QJ.3803

IDIER D., PARIS F., LE COZANNET G., *et al.* (2017). *Sea-level rise impacts on the tides of the European Shelf,* Continental Shelf Research, 137(January), pp 56–71. doi:10.1016/j.csr.2017.01.007

IDIER D., DUMAS F., MULLER H. (2012). *Tide-surge interaction in the English Channel,* Natural Hazards and Earth System Science, 12(12), pp 3709–3718. doi:10.5194/nhess-12-3709-2012

MÜLLER M. (2011). *Rapid change in semi-diurnal tides in the North Atlantic since 1980,* Geophysical Research Letters, 38(11), pp 1–6. doi:10.1029/2011GL047312

PELLING H.E., GREEN J.A.M. (2014). *Impact of flood defences and sea-level* rise on the European Shelf tidal regime, Continental Shelf Research, 85, pp 96–105. doi:10.1016/j.csr.2014.04.011

PELLING H.E., UEHARA K., GREEN J.A.M. (2013). *The impact of rapid coastline changes and sea level rise on the tides in the Bohai Sea, China,* Journal of Geophysical Research: Oceans, 118(7), pp 3462–3472. doi:10.1002/jgrc.20258

POUVREAU N., MIGUEZ B.M., SIMON B., WÖPPELMANN G. (2006). *Évolution de l'onde semi-diurne M2 de la marée à Brest de 1846 à 2005'*, Comptes Rendus - Geoscience, 338(11), pp 802–808. doi:10.1016/j.crte.2006.07.003

RAY R.D. (2006). *Secular changes of the M2 tide in the Gulf of Maine,* Continental Shelf Research, 26(3), pp 422–427. doi:10.1016/j.csr.2005.12.005

SCHWARZ G. (1978). *Estimating the Dimension of a Model,* The Annals of Statistics, 6(2). pp 461-464. doi:10.1214/aos/1176344136

WOODWORTH P.L. (2010). *A survey of recent changes in the main components of the ocean tide*, Continental Shelf Research, 30(15), pp 1680–1691. doi:10.1016/j.csr.2010.07.002

WOODWORTH P.L., SHAW S.M., BLACKMAN D.L. (1991). *Secular trends in mean tidal range around the British Isles and along the adjacent European coastline,* Geophysical Journal International, 104(3), pp 593–609. doi:10.1111/j.1365-246X.1991.tb05704.x

YAMAGUCHI R., SUGA T. (2019). *Trend and Variability in Global Upper-Ocean Stratification Since the 1960s*, Journal of Geophysical Research: Oceans, 124(12), pp 8933–8948. doi:10.1029/2019JC015439